

# Spectral properties of La/B - based multilayer mirrors near the boron K absorption edge

Igor A. Makhotkin,<sup>1,\*</sup> Erwin Zoethout,<sup>1</sup> Eric Louis,<sup>1</sup> Andrei M. Yakunin,<sup>2</sup> Stephan Müllender,<sup>3</sup> and Fred Bijkerk<sup>1,4</sup>

<sup>1</sup>FOM Institute DIFFER - Dutch Institute for Fundamental Energy Research, Nieuwegein, the Netherlands

<sup>2</sup>ASML, Veldhoven, the Netherlands

<sup>3</sup>Carl Zeiss SMT GmbH, Oberkochen, Germany

<sup>4</sup>MESA + Institute for Nanotechnology, University of Twente, Enschede, the Netherlands

\*I.A.Makhotkin@diffier.nl

**Abstract:** The spectral properties of La/B, La/B<sub>4</sub>C, and LaN/B, LaN/B<sub>4</sub>C multilayer mirrors have been investigated in the 6.5-6.9 nm wavelength range based on measured B and B<sub>4</sub>C optical constants. Experimentally it is verified to what extent measured and tabulated optical constants are applicable for simulations of the reflectivity of these short period multilayer mirrors. The measured maximum reflectance at various wavelength values around the boron-K absorption edge is compared to calculated values from model systems. The measured reflectance profiles of La/B and La/B<sub>4</sub>C show a maximum at a slightly larger wavelength than calculations would predict based on the measured B and B<sub>4</sub>C optical constants. This is explained by the influence of a formed boron-lanthanum compound on the wavelength where the multilayer shows maximum reflectance. The maximum reflectance profiles of LaN/B and LaN/B<sub>4</sub>C multilayers can be described accurately by using the same boron atomic scattering factors, indicating boron in the LaN/B<sub>4</sub>C multilayer to be in a similar chemical state as boron in the LaN/B multilayer. It also indicates that nitridation of the La layer in the multilayer prevents the formation of La-B compounds. We show that the optimal wavelength for boron based optics is about 6.65 nm and depends on the B chemical state. Finally, using the measured B optical constants we are able to calculate the spectral response of the multilayers, enabling the prediction of the optimal parameters for the above mentioned multilayers

©2012 Optical Society of America

**OCIS codes:** (340.7480) X-rays, soft x-rays, extreme ultraviolet (EUV); (340.7470) X-ray mirrors.

---

## References and links

1. A. M. Hawryluk and N. M. Ceglio, "Wavelength considerations in soft-x-ray projection lithography," *Appl. Opt.* **32**(34), 7062–7067 (1993).
2. A. V. Vinogradov, I. A. Brytov, A. Ya. Grudskii., M. X. Kogan, and I. V. Kozhevnikov, *Zerkal'naya rentgenovskaya optika (X-ray Mirror Optics, Leningrad: Mashinostroenie, 1989).*
3. E. Spiller, *Soft X-ray Optics* (SPIE Optical Engineering press, 1994).
4. T. Tsarfati, R. W. E. van de Kruijs, E. Zoethout, E. Louis, and F. Bijkerk, "Reflective multilayer optics for 6.7 nm wavelength radiation sources and next generation lithography," *Thin Solid Films* **518**(5), 1365–1368 (2009).
5. C. Montcalm, P. A. Kearney, J. M. Slaughter, B. T. Sullivan, M. Chaker, H. Pépin, and C. M. Falco, "Survey of Ti-, B-, and Y-based soft x-ray-extreme ultraviolet multilayer mirrors for the 2- to 12-nm wavelength region," *Appl. Opt.* **35**(25), 5134–5147 (1996).
6. J. M. André, P. Jonnard, C. Michaelsen, J. Wiesmann, F. Bridou, M. F. Ravet, A. Jerome, F. Delmotte, and E. O. Filatova, "La/B<sub>4</sub>C small period multilayer interferential mirror for the analysis of boron," *XRay Spectrom.* **34**(3), 203–206 (2005).
7. S. Andreev, M. Barysheva, N. Chkhalo, S. Gusev, A. Pestov, V. Polkovnikov, D. Rogachev, N. Salashchenko, Y. Vainer, and S. Zuev, "Multilayer x-ray mirrors based on La/B<sub>4</sub>C and La/B<sub>9</sub>C," *Tech. Phys.* **55**(8), 1168–1174 (2010).

8. S. S. Andreev, M. M. Barysheva, N. I. Chkhalo, S. A. Gusev, A. E. Pestov, V. N. Polkovnikov, N. N. Salashchenko, L. A. Shmaenok, Y. A. Vainer, and S. Y. Zuev, "Multilayered mirrors based on La/B<sub>4</sub>C(B<sub>9</sub>C) for X-ray range near anomalous dispersion of boron ( $\lambda \approx 6.7$  nm)," *Nucl. Instrum. Methods Phys. Res. A* **603**(1-2), 80–82 (2009).
9. T. Tsarfati, R. W. E. van de Kruijs, E. Zoethout, E. Louis, and F. Bijkerk, "Nitridation and contrast of B<sub>4</sub>C/La interfaces and X-ray multilayer optics," *Thin Solid Films* **518**(24), 7249–7252 (2010).
10. S. S. Churilov, R. R. Kildiyarova, A. N. Ryabtsev, and S. V. Sadovsky, "EUV spectra of Gd and Tb ions excited in laser-produced and vacuum spark plasmas," *Phys. Scr.* **80**(4), 045303 (2009).
11. E. Spiller, "Refractive index of amorphous carbon near its K-edge," *Appl. Opt.* **29**(1), 19–23 (1990).
12. D. Ksenzov, T. Panzner, C. Schlemper, C. Morawe, and U. Pietsch, "Optical properties of boron carbide near the boron K edge evaluated by soft-x-ray reflectometry from a Ru/B(4)C multilayer," *Appl. Opt.* **48**(35), 6684–6691 (2009).
13. D. Ksenzov, C. Schlemper, and U. Pietsch, "Resonant soft x-ray reflectivity of Me/B(4)C multilayers near the boron K edge," *Appl. Opt.* **49**(25), 4767–4773 (2010).
14. A. V. Vinogradov and B. Y. Zeldovich, "X-ray and far uv multilayer mirrors: principles and possibilities," *Appl. Opt.* **16**(1), 89–93 (1977).
15. B. L. Henke, E. M. Gullikson, and J. C. Davis, "X-Ray interactions: photoabsorption, scattering, transmission, and reflection at E = 50–30,000 eV, Z = 1–92," *At. Data Nucl. Data Tables* **54**(2), 181–342 (1993).
16. E. Gullikson, web site The Center for X-Ray Optics (1995–2010), retrieved [http://henke.lbl.gov/optical\\_constants/](http://henke.lbl.gov/optical_constants/).
17. D. Ksenzov, "Interaction of femtosecond x-ray pulses with periodical multilayer structures," (PhD Thesis, Siegen University, Siegen, 2010).
18. M. Fernández-Perea, J. I. Larruquert, J. A. Aznárez, J. A. Méndez, M. Vidal-Dasilva, E. Gullikson, A. Aquila, R. Soufli, and J. L. G. Fierro, "Optical constants of electron-beam evaporated boron films in the 6.8–900 eV photon energy range," *J. Opt. Soc. Am. A* **24**(12), 3800–3807 (2007).
19. R. Soufli, A. L. Aquila, F. Salmassi, M. Fernández-Perea, and E. M. Gullikson, "Optical constants of magnetron-sputtered boron carbide thin films from photoabsorption data in the range 30 to 770 eV," *Appl. Opt.* **47**(25), 4633–4639 (2008).
20. Z. Jiang, Toolbox: X-ray Refraction of Matter, MatLab Central, (2004).
21. E. Louis, A. E. Yakshin, T. Tsarfati, and F. Bijkerk, "Nanometer interface and materials control for multilayer EUV-optical applications," *Prog. Surf. Sci.* **86**(11-12), 255–294 (2011).
22. D. L. Windt, "IMD - Software for modeling the optical properties of multilayer films," *Comput. Phys.* **12**(4), 360–370 (1998).
23. F. Scholze, C. Laubis, C. Buchholz, A. Fischer, S. Plöger, F. Scholz, H. Wagner, and G. Ulm, "Status of EUV reflectometry at PTB," *Proc. SPIE* **5751**, 749–758 (2005).
24. M. Born and E. Wolf, *Principles of Optics*, 7th ed. (Cambridge university press, Cambridge, 2000).
25. L. G. Parratt, "Surface studies of solids by total reflection of x-rays," *Phys. Rev.* **95**(2), 359–369 (1954).
26. G. H. Kwei and B. Morosin, "Structures of the boron-rich boron carbides from neutron powder diffraction: implications for the nature of the inter-icosahedral chains," *J. Phys. Chem.* **100**(19), 8031–8039 (1996).

## 1. Introduction

Optics for extreme ultraviolet radiation of 6.5–6.9 nm wavelength is interesting for many applications. For example a new generation photolithography or free electron lasers requires optics that reflects at these wavelengths.

It is shown [1–5] that around 6.6 nm wavelength the highest normal incidence reflectance is obtained with multilayer mirrors based on lanthanum as reflector and boron as spacer material. Boron is the appropriate spacer material because of the close proximity to the boron K-absorption edge. In previous work La/B<sub>4</sub>C multilayers have been studied [6–8], replacing boron with B<sub>4</sub>C to simplify the deposition process. Measured EUV reflectance from real La/B<sub>4</sub>C multilayers is significantly lower than the value predicted theoretically for ideal structures. One of the factors limiting the EUV reflectance is intermixing at the interfaces between La and B. It has been shown [9] that nitridation of the La layer can reduce intermixing by formation of the chemically stable LaN compound.

A wavelength dependent reflectivity study of multilayers is interesting from both applied and fundamental point of view, particularly since key in designing the next generation EUVL optics will be the matching of its optimum wavelength to that of the candidate EUV sources based on Tb or Gd. The published emission spectra from these materials show the highest intensities at 6.52 and 6.78 nm respectively [10]. To find optimal matching of optics and sources, knowledge of wavelength dependent reflectance is required. On the other hand,

multilayer reflectivity spectra recorded in the vicinity of the B absorption edge hold information about the B chemical state inside the multilayer [11–13].

Here we have studied spectral properties of La-/B- based multilayers with four different layer compositions: La/B, La/B<sub>4</sub>C, LaN/B and LaN/B<sub>4</sub>C. We propose a way to predict the behavior of model structures for these multilayers. Two major factors determine the multilayer reflectivity profile: the optical constants of the materials in the multilayers and the structure of the multilayers. In this paper we mainly examine the influence of the B optical constants on the La-/B- based multilayer reflectivity profile. The theoretical description of the wavelength dependency of the multilayer reflectivity matches the measured values for all material combinations best when using the measured boron optical constants, thus enabling the prediction of the optimal multilayers parameters and the theoretical maximum reflectivity for La/B, La/B<sub>4</sub>C, LaN/B and LaN/B<sub>4</sub>C multilayer mirrors.

## 2. Application of measured optical constants for simulation of multilayer reflectivity

In resonant Bragg conditions the multilayer mirror peak reflectance can be calculated analytically [2,14]. We consider mirrors with sufficient film thickness to show no influence of the substrate material on the reflectance. The multilayer peak reflectance mainly depends on the optical contrast between reflector and spacer. Boron has been chosen as a spacer because of its extremely low absorption in the vicinity of its absorption edge at 188 eV (or 6.6 nm). Lanthanum is chosen as reflector for its optical contrast with B and low absorption at this wavelength range. A maximum amount of bi-layers is now contributing to the constructive interference that forms the peak reflectance.

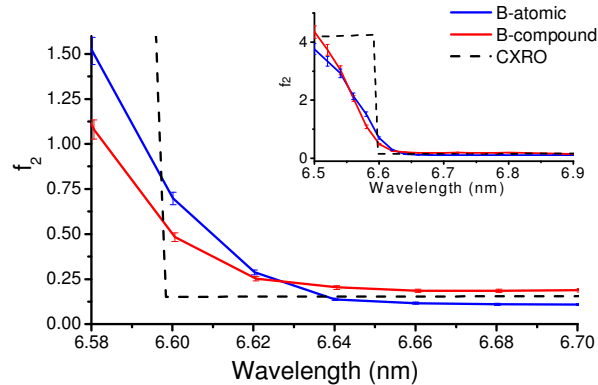


Fig. 1. Boron atomic scattering factors obtained from a B film (B-atomic) [18], a B<sub>4</sub>C film (B-compound) [19] and the CXRO database [15]

The most complete database of optical constants in the soft and hard X-ray wavelength range has been published by Henke et.al [15]. and can be obtained from the Centre for X-Ray Optics (CXRO) web site [16]. Henke optical constants work perfectly for wavelengths far from the absorption edges. Therefore, the CXRO database can be used for La, but for boron in the 6.x nm wavelength range the optical constants can be less accurate since there are only two values of boron atomic scattering factors measured near 6.6 nm, namely at 6.44 and 6.76 nm. All other plotted values have been calculated [15]. Possible shifts of the boron absorption edge due to chemical interaction to foreign species, for example carbon, cannot be taken into account in calculations. Furthermore the used layer thickness of 1.5 nm is of the same order as the thickness of the interfaces (approximately 1 nm), indicating that in case of interface compound formation (here most likely LaB<sub>6</sub>) it will occupy most of the spacer layer volume and will thus affect the optical constants. For example Ksenzev, using a photon-in-photon-out

technique [12], found that the difference of the B adsorption edge in Ru/B<sub>4</sub>C and W/B<sub>4</sub>C multilayers is 1 eV [17].

In this work we have used measured B [18] and B<sub>4</sub>C [19] optical constants. Pure boron optical constants have been calculated through transmission measurements of thick e-beam deposited B films (29, 58 and 93 nm) deposited onto a C coated grid. The optical constants of magnetron deposited B<sub>4</sub>C films have been similarly calculated from the transmission measurements on films with thicknesses of 54, 79 and 112 nm. In both cases, the use of three different thicknesses enabled excluding effects of surface oxidation [18,19].

$$\begin{aligned}
 n &= 1 - \delta + i\beta \\
 \delta &= \frac{r_0 \lambda^2}{2\pi} \frac{\rho N_A}{MW} \sum_i n^i f_1^i \\
 \beta &= \frac{r_0 \lambda^2}{2\pi} \frac{\rho N_A}{MW} \sum_i n^i f_2^i
 \end{aligned} \tag{1}$$

The optical constants of mixed materials, based on compound composition and density, and knowing the real ( $f_1$ ) and imaginary ( $f_2$ ) part of the atomic scattering factors of the materials, can be calculated according to Eq. (1). To extract the B scattering factors in the B<sub>4</sub>C compound of the measured B<sub>4</sub>C films [19], carbon and oxygen have to be taken into account since they account for a significant amount of the sample volume. This model of B atomic scattering factors is labeled as B-compound model. Models with B atomic scattering factors reconstructed from the measured B film are labeled B-atomic model. The CXRO database is used for the scattering factors of elemental materials with absorption edges far from our wavelength range (6.5-6.9 nm). The presence of C and O by itself has almost no influence on the wavelength dependent boron optical constants in a B<sub>4</sub>C compound, except that the presence of O and C increases the absorption of the spacer layer (A possible shift of B optical constants due to boron oxide or boron carbide formation is not considered here yet). Figure 1 shows the calculated B atomic scattering factors  $f_2$  from the boron and B<sub>4</sub>C film together with data from the CXRO database. There is a noticeable difference in the absorption onset: in the B<sub>4</sub>C film the B absorption edge is shifted 0.02 nm (or 0.6 eV) to a shorter wavelength with respect to the B film. This shift is the result of the B electron binding energy chemical shift that is a consequence of the boron carbide formation. The error bars in Fig. 1 indicate the uncertainty in the determination of the film density. The wavelength accuracy is determined by the photon energy accuracy which is 0.007% [19] or 0.4 pm for 6 nm radiation.

To illustrate the influence of different chemical states of B on the multilayer reflectivity, La/B<sub>4</sub>C peak reflectance spectra have been calculated for multilayer structures without roughness or intermixing and are shown in Fig. 2. The two different data sets are used to reconstruct the B<sub>4</sub>C optical constants. First, the Soufli et al. [19] measured B<sub>4</sub>C optical constants (indicated as B-compound), and second, a mix model of 4B + 1C (indicated as B-atomic) with the optical constants calculated [20] according to Eq. (1), using data of a B film measured by Fernandez et al [18]. Finally, the optical constants for 4B + 1C are calculated with B and C atomic scattering factors obtained from the CXRO database [15] (B<sub>4</sub>C (CXRO)). Similar to Fig. 1 it is observed that the wavelength of maximum reflectance is 0.02 nm longer for B<sub>4</sub>C (B-atomic) than for B<sub>4</sub>C (B-compound). Both reflectivity spectra calculated from measured optical constants are shifted to longer wavelength with respect to calculations based on CXRO data. The most striking difference between database and the measured optical constants in Fig. 1 and 2 is observed around the absorption edge. Where the CXRO data shows a steep drop in reflectance for a wavelength below the edge, the measured data result in a more gradual drop in reflectance.

For longer wavelength, further from the absorption edge, the value of the multilayer reflectance calculated using the B-atomic model is slightly higher than when the B-compound

model is used. The boron chemical state cannot influence the absolute level of reflectance far from the absorption edge. The difference can be explained assuming an error in the film density, or the determination of the  $B_4C$  or B film composition.

To assess the validity of the measured optical constants for our multilayers, we have performed a set of reflectivity spectral measurements of La-/B- based multilayers at different angles of incidence that allows us to study multilayer reflectivity at different wavelength, a method described by Spiller [11]. These measurements are described in section 4 of this paper.

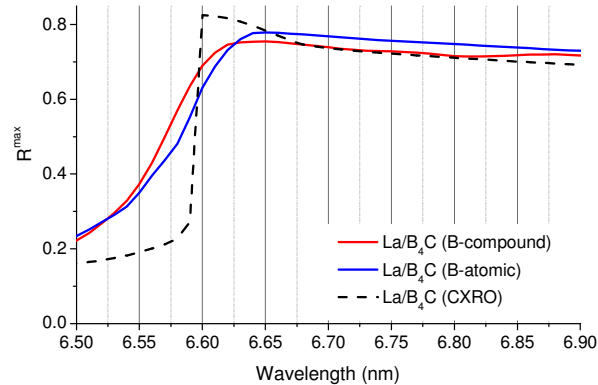


Fig. 2. Analytical calculation of a perfect La/ $B_4C$  multilayer for different  $B_4C$  optical constants, namely – measured  $B_4C$  optical constants (B-compound) [19], measured B atomic scattering factors used to calculate  $B_4C$  optical constants (B-atomic) [18] and values calculated from elemental data from ref [15].

### 3. Experimental

La/B, La/ $B_4C$  and LaN/B, LaN/ $B_4C$  multilayers consisting of 50 bi-layers, with a bi-layer thickness of approximately 4 nm have been made in an UHV environment of  $1.10^{-8}$  mbar [21]. La, B and  $B_4C$  layers were deposited at room temperature using electron beam evaporation. LaN was prepared by low energy N-ion post treatment of each La layer. Layer thicknesses were controlled by quartz crystal oscillator microbalances. Natively oxidized super polished Si wafers have been used as substrate.

For comparison with the measured data, the simulations of the reflectance of the different multilayer compositions described in the next chapter require individual models. Initially the models contain 50 equal bi-layer periods with layer thickness based on the quartz crystal oscillator microbalance values obtained during coating. Furthermore, the bulk values of material density are used. To improve these initial models each deposited multilayer was characterized using grazing incidence hard x-ray (Cu- $K_\alpha$ ) angular dependent reflectance measurements (GI-XRR). Calculated GI-XRR spectra were fit to the measured spectra using IMD [22] and similar homemade software. In the modeling the optical constants are calculated using the Mat Lab toolbox [20] and interface roughness is taken into account by applying the Debby-Waller factor. Layer thickness, density and interface roughness were the free parameters during fitting. The reflectance around 6.6 nm has been measured at the beam line of the Physikalisch Technische Bundesanstalt (PTB, Berlin) at the BESSY II synchrotron radiation source using sigma-polarized soft X-ray radiation. The measurement setup has a relative uncertainty of the intensity measurements equal to 0.14%. The wavelength determination is accurate within 0.014% or 0.9 pm for 6.6 nm [23].

GI-XRR and soft X-rays normal incidence reflection are sensitive to different multilayer parameters. GI-XRR is more sensitive to layer roughness and individual layer thickness,

while soft X-ray reflection is more sensitive to layer density and layer composition. Hard X-ray reflectivity data alone has not been sufficient to provide a model that would fit the measured soft X-ray reflection, not even far from the absorption edge, where there is no significant influence of the B chemical state. Models for simulation of the soft X-ray reflectivity at different angles of incidence have been fitted to soft X-ray reflection spectra recorded at  $1.5^\circ$  of normal incidence. The models obtained from GI-XRR data fitting served as starting points for soft X-ray reflectance data fitting.

Unlike calculations presented in the first section, where simplified analytical dependencies are used, the experimental data have been simulated using the Fresnel matrix formalism optimized for periodic bi-layer structures [24].

#### 4. Measurements and analysis

For all four multilayers described in the previous section, wavelength depended reflectance spectra have been measured at various angles of incidence. In order to reduce the large amount of soft X-ray reflectance data, the maximum reflectance and the corresponding wavelength at which this reflectance occurs were determined for each wavelength scan. Furthermore, each wavelength of maximum reflectance has been simulated using the model described above. Figure 3 presents a comparison of measured and simulated results normalized to the highest reflectance in the wavelength plot.

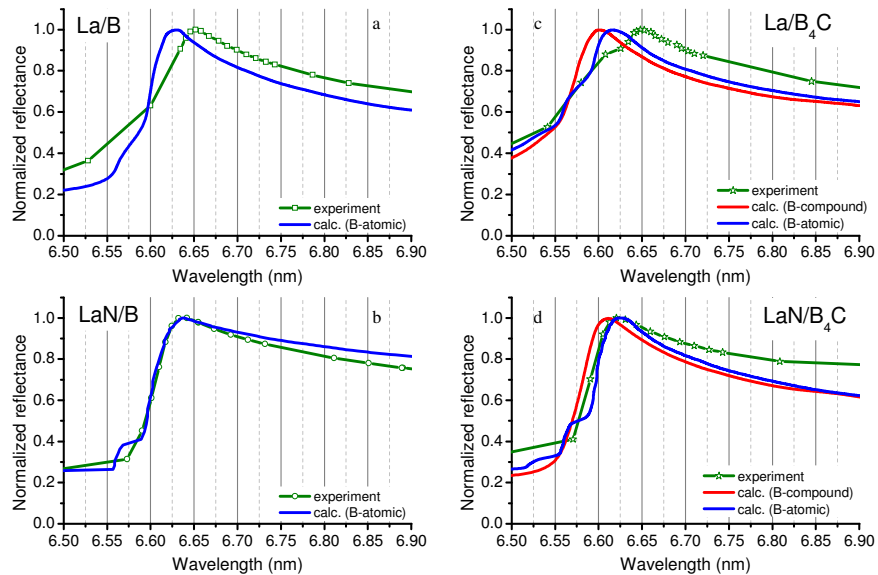


Fig. 3. Normalized maximum reflectance of measured samples and calculations using measured boron and  $B_4C$  optical constants

Figure 3(a) shows that the simulated La/B reflectivity profile shows a maximum at a wavelength that is 0.02 nm lower than experimentally observed. Figure 3(b) however shows that there is no significant shift between the measured and calculated reflectivity profiles of LaN/B multilayer. The observed shift in the La/B case can only be explained by a change in the boron optical constants induced by a chemical shift of the B-K electron binding energy, most likely due to La-B compound formation, probably  $LaB_6$ . The similar shape and position of the calculated and measured reflectivity profiles of LaN/B multilayers indicate that in this material combination the B atoms remain in the atomic state, proving that nitridation of the La layers reduces the intermixing of lanthanum and boron. Furthermore, for the wavelength range shorter than where the maximum reflectance occurs, a clear mismatch of experimental

and calculated data is observed for La/B (Fig. 3(a)): around 6.60 nm the curves cross, hinting that part of the boron might still be in an elemental state.

For the LaN/B combination (Fig. 3(b)) at longer wavelength, a different slope is observed. This is a consequence of a deviation of the model and the real multilayer structure. Probably in this case the accuracy of determination of the lanthanum content per bi-layer and the thickness of the intermixed zone at the interfaces is not sufficient to reconstruct the shape of the reflectivity profile. This type of model variations can slightly change the slope of the reflectance profile, but cannot change the position of the reflectance maximum more than 0.005 nm.

A more complicated picture is observed in the La/B<sub>4</sub>C reflectivity profile. Figure 3(c) shows the presence of at least two distinct wavelengths pointing to absorption edge phenomena. The maximum reflectance of the experimental data in Fig. 3(c) is at the same position as in La/B profile of Fig. 3(a), indicating similar La-B compound formation resulting in a B absorption edge around 6.65 nm. The shape of the measured reflectivity profile in the wavelength range below the reflectance maximum can be explained by the presence of the B atoms in a different chemical state, resulting in absorption edge phenomena at a shorter wavelength than 6.65 nm. Calculations have been performed with two sets of optical constants: B<sub>4</sub>C-(B-atomic) and B<sub>4</sub>C-(B-compound). Comparing experimental values to both calculations, the second absorption edge in the experiment is closer to the B<sub>4</sub>C-(B-atomic) model than to the B<sub>4</sub>C-(B-compound), although a mix of more than two species cannot be excluded. Therefore we suggest that at least part of the boron is in the elemental state. Figure 3(d) shows the results of the LaN/B<sub>4</sub>C multilayer together with the B<sub>4</sub>C-atomic and compound models. Remarkably the profile of the experiment curve matches nicely with the B<sub>4</sub>C-(B-atomic) model but less accurate to the B<sub>4</sub>C-(B-compound) model. Since the LaN used in Fig. 3(b) is the same as in Fig. 3(d), it is assumed that nitridation reduces the intermixing at the interfaces significantly in both cases. This would imply that the boron in the B<sub>4</sub>C layers has a similar optical response as the measured boron film, probably because it is in an elemental state. This would imply that the B<sub>4</sub>C layer is more a mix of B and C, rather than the B<sub>4</sub>C compound. Figure 3 shows that the optical response of lanthanum-boron based multilayers is complex and cannot be predicted accurately enough from database values. The exact composition and chemical interaction of these nanometer thin layers determines the optical response near the absorption edge and therefore the optimum performance in any application.

## 5. Theoretical optimization

Different applications can pose different requirements on the optics. For example, the use of multilayer mirrors as monochromator for soft X-ray radiation requires high peak reflectivity in combination with a small bandwidth, while projection photolithography requires high integrated reflectance from the stack of several mirrors over a certain bandwidth.

In this section we present a theoretical optimization of the four material combinations, La/B, La/B<sub>4</sub>C and LaN/B, LaN/B<sub>4</sub>C, in terms of the maximum achievable reflectance and the corresponding wavelength for an angle of incidence of 1.5° with respect to the surface normal.

Although we were not able to perfectly fit the measured reflectivity profiles with B and B<sub>4</sub>C optical constants measured from thick films, the match is good enough to use them to investigate the multilayer composition that would perform best in the vicinity of the B absorption edge. In the previous section the best fit of the measured reflectivity profiles is obtained using B atomic scattering factors calculated from a measured boron film. These scattering factors are used here for B and for B<sub>4</sub>C in modeling multilayers.

In general the bi-layer thickness ( $\Lambda$ ) determines the wavelength of maximum reflectance. However, the reflector to bi-layer thickness ratio  $\Gamma$  can affect both the maximum reflectivity as well as the width of the reflectance peak, represented by the full width at half the

maximum value (FWHM). In this section we optimized the  $\Gamma$  ratio as well as the number of bi-layers required to have the highest reflectance values. This is a different situation than in the previous section where we modeled the actually deposited multilayers. Therefore, the wavelength of maximum reflectance for the optimized multilayers in this section can deviate from the data presented in Fig. 3.

The results of optimization for different multilayer compositions are presented in Table 1. As in the previous section, calculations use the Fresnel matrix formalism optimized for ideal periodic bi-layer structures [24].

**Table 1. Calculated Parameters of the Optimized Multilayers.**

ML composition	$\Gamma, d_{La}/\Lambda$	$\Lambda, \text{nm}$	Optimal wavelength, nm	Period number	$R^{\text{max}}, \%$	FWHM @ optimal wavelength, nm.
La/B	0.39	3.34	6.66	175	82.5	0.070
LaN/B				160	82	0.076
La/B <sub>4</sub> C	0.41		6.65	185	77.5	0.060
LaN/B <sub>4</sub> C				170	77.5	0.066

The table shows that optimum  $\Gamma$  for B<sub>4</sub>C based multilayers is slightly higher than for B-based multilayer, which is attributed to the larger absorption in B<sub>4</sub>C.

The presence of nitrogen in the La layers has almost no influence on the multilayer spectral properties and optimal parameters except for the amount of periods. To obtain optimized reflectance in LaN/B based multilayer requires 15 periods less than for La/B, which is the result of the slightly more favorable optical constants of LaN. The reduced optimal number of periods for LaN explains the slight increase in FWHM of these multilayers.

Table 1 also shows that B-based multilayers have a higher maximum reflectance than B<sub>4</sub>C-based multilayers. The reason for this is that C in B<sub>4</sub>C results in a high absorption of the spacer layer. Since the same scatter factors are used to calculate the boron or B<sub>4</sub>C layers no significant difference in critical wavelength is observed. The minor shift of the optimal wavelength of B<sub>4</sub>C based multilayers with respect to B-based multilayers can be explained by the change in optical contrast in the multilayers due to presence of C, resulting in a different optimum  $\Gamma$ .

The presented calculations for optimized reflectance can serve as a starting point to obtain maximum reflectance experimentally. However, in this section we ignored the influence of interface imperfections on the multilayer reflectivity profile, as well as possible compound formation. As we experimentally showed in the previous section, compound formation can explain the shift of the optimal wavelength.

## 6. Discussion

In the first section, analytical formulas have been used where in the optimization section the matrix formalism has been applied. Both approaches are able to calculate reflectance spectra as well as peak reflectance and FWHM. When only optimization of peak reflectance is required, it is much faster to use the analytical approach, but for determining the exact shape of the peak it lacks accuracy and the matrix formalism or recursive Parratt equations [25] should be employed.

In photolithography, optimizing the multilayer mirror performance is required to match the reflectivity spectra with the source emission and photo resist absorption spectra. Reversely, the performance of possible mirrors is input in selecting the source. The convolution of source spectrum and mirror reflectance determines the best combination.

Calculated ideal reflectivity spectra show that the optimal source wavelength should be around 6.66 nm. For a wavelength larger than 6.66 nm there is only a weak dependency on



the wavelength, whereas for smaller wavelength, crossing the boron edge, the reflectance drops dramatically. For example decreasing the wavelength to 6.60 nm will reduce the reflectance to 40% of the optimal reflectivity. In the experimental section, from multilayer reflectivity profiles it is observed that a pronounced maximum between 6.62 and 6.66 nm exists, where the exact optimal wavelength depends on the B compound.

As discussed in section 4, the optical properties in the vicinity of the B-absorption edge of our thin B<sub>4</sub>C layers in the multilayer stack show clear similarities with B in a thick film, rather than with the optical properties of a B<sub>4</sub>C film, which could be an indication that part of the B is in its elemental state. This can be understood since boron carbide with the B<sub>4</sub>C stoichiometry is a complex material consisting of B<sub>11</sub>C icosahedra and C-B-C chains [26]. Most likely the B<sub>4</sub>C layer thickness (~2 nm) in the multilayer is not enough to form this complex B<sub>4</sub>C structure. The detailed study of the chemical interactions in La-B<sub>4</sub>C systems, including the influence of nitridation, will be topic of future studies.

The observed dependency of the critical wavelength on the B chemical compound can be associated with a shift of the B-1s electron binding energy. Our X-ray photoelectron spectroscopy analysis has shown that this electron binding energy in a lanthanum-boride shifts to lower energy with respect to bulk B and to higher energy when B resides in a thick film of boron-carbide. The influence of chemical bonds on the B-1s electron binding energy opens possibilities to shift the optimal wavelength to smaller values by replacing B with a compound with a larger B-1s electron binding energy, which is the case in for example BN.

## Conclusions

It has been shown that for simulations of the multilayer reflectivity of La/B, La/B<sub>4</sub>C, LaN/B and LaN/B<sub>4</sub>C systems near the boron absorption edge, the boron chemical state has to be taken into account. From experimental data of La/B and La/B<sub>4</sub>C multilayers it is observed that a significant amount of boron is probably bound to La. This results in a shift of the B absorption edge to a longer wavelength, which significantly changes the optical properties. The reflectivity of LaN/B and LaN/B<sub>4</sub>C multilayers can be well described by using the measured atomic B optical constants, which suggests that in both multilayers boron atoms are in a similar state as in a boron film. In our case, for the calculation of the reflectance of short period La/B<sub>4</sub>C and LaN/B<sub>4</sub>C multilayers, it is best to use the B scattering factors to simulate B<sub>4</sub>C optical constants instead of using measured B<sub>4</sub>C optical constants.

Numerical analysis has shown that maximum reflectance can be obtained for B-based multilayers near  $\lambda = 6.66$  nm. However, the influence of the actual multilayer structure, like interface imperfections and ultra-thin film chemical composition, may shift the optimal wavelength in both directions.

## Acknowledgments

This work is part of the research project 'Multilayer Optics for Lithography Beyond the Extreme Ultraviolet Wavelength Range' carried out with financial support of the Dutch Technology Foundation (STW), in the frame of the programme on Thin Film Nanomanufacturing. This work is also a part of the research programme 'Controlling photon and plasma induced processes at EUV optical surfaces (CP3E)' of the 'Stichting voor Fundamenteel Onderzoek der Materie (FOM)' with financial support from the 'Nederlandse Organisatie voor Wetenschappelijk Onderzoek (NWO)'. The CP3E programme is co-financed by Carl Zeiss SMT and ASML, and the AgentschapNL through the EXEPT program. The authors are grateful to the Physikalisch Technische Bundesanstalt (PTB, Berlin, Germany) for soft X-ray and EUV reflectance measurements and to Regina Soufli and Mónica Fernández-Perea (Lawrence Livermore National Laboratory, Livermore, California) for providing B and B<sub>4</sub>C measured optical constants data for our analysis.